On-demand manufacture of circular 3D-printable resins†

Nailah N. Moghal,[a] Daniele Giannantonio, [iD][a] Megan R. Elliott,[a] Neha Mehta,[b] Andrew P. Dove [iD] *[a] and Arianna Brandolese [iD] *[a]

Recent progress in circular 3D-printable photocurable resins that enable closed-loop recycling marks a significant step forward in reducing wasteful manufacturing methods and non-recyclable printed plastics. However, with 3D printing technologies shifting from prototyping to full-scale production, the demand for high-scale processes and easily tuneable resin compositions can benefit from the design of automated systems. Herein, we report on the on-demand preparation of a circular 3D-printable resin, achieved through a continuous flow approach. A supported enzyme (Lipase B from *Candida antarctica*) was used to promote a green esterification of the lipoic acid with biobased alcohols to prepare circular biobased photocurable resins. The supported enzyme was employed for the preparation of a packed bed reactor and was easily recycled and reused to achieve the continuous production of lipoate-based photocurable resins with tuneable composition. Lastly, the environmental impact of the developed on-demand manufacturing process was compared to the previously reported esterification protocols through life cycle assessment, showing the effectiveness of continuous enzymatic flow synthesis in enhancing environmental performance across multiple areas, from human health to ecosystem impact and resources.

Introduction

Vat photopolymerisation is a widely adopted additive manufacturing (3D printing) method that relies on light-activated polymerisation to selectively solidify liquid resins held in a vat.[1,2] The additive manufacturing market, currently valued at $0.9 billion, accounts for a significant share of the broader photopolymer market, which exceeds $2.8 billion in total, and it is projected to expand at a compound annual growth rate of 16.9% as photopolymer-based 3D

[a]*University of Birmingham, School of Chemistry, Edgbaston, B15 2TT, UK. E-mail: a.brandolese@bham.ac.uk; a.dove@bham.ac.uk*

[b]*University of Birmingham, School of Chemical Engineering, Birmingham Energy Institute, Edgbaston, B15 2TT, UK*

printing technologies become faster and shift from prototyping to full-scale production.[3] However, this growth must be accompanied by advancements in photopolymer resin technology to ensure that additive manufacturing contributes to a truly sustainable and circular plastic economy.

Most resin components are derived from non-renewable fossil resources, and many resin-based processes generate waste in the form of partially cured material that cannot be reused.[4–7] Additionally, the majority of 3D-printed objects made from permanently cross-linked resins are neither degradable nor recyclable, further exacerbating environmental damage and creating significant end-of-life challenges. To tackle this issue, closed-loop recycling of 3D-printed polymers, in which the printed material is fully depolymerised to a resin and re-printed, has been explored. Circular photocurable resins have been focused on the introduction of dynamic bonds that can break down under certain conditions within permanently cross-linked polymer networks, allowing partial depolymerisation of printed parts.[8–16] Recently, we reported on circular lipoate-based resins entirely obtained from renewable feedstocks that can be 3D-printed into high-resolution parts, efficiently deconstructed, and subsequently reprinted in a circular manner.[11] Yang *et al.* have also reported a circular additive manufacturing process to produce high-performance polymer parts containing dithioacetal bonds that can be decomposed into reprintable liquid resins under a specific condition.[16]

3D printing has been successfully employed to prepare sophisticated architectures in flexible devices and multimaterial objects that can have varied properties, including conductivity, self-healing capacity, and recyclability.[17–19] Through vat photopolymerisation, it is possible to achieve the rapid production of customised 3D-printed components. Tuneable resins are conventionally formulated by varying the ratio of monomer manually,[20,21] whereas the need to move to a large-scale production and the demand for precise control over resin composition can benefit from the design of automated systems. In this regard, the flow approach can be leveraged to develop an automated method to prepare photocurable resins with easily tuneable composition. Applying flow chemistry techniques to synthesis offers several advantages over traditional batch synthesis methods.[22–25] Not only does it allow for greater repeatability and easier scale-up, but it can also be tuned to deliver bespoke products (*e.g.* resin with specific composition).[26,27] While flow chemistry has largely benefited from the use of 3D printing (*e.g.* to print continuous flow reactors),[28] there have been no reports of using flow systems to directly synthesise photopolymer resins for 3D printing.

Herein, we report on the preparation of an on-demand circular biobased resin by leveraging continuous flow production (Fig. 1). Lipoate-based
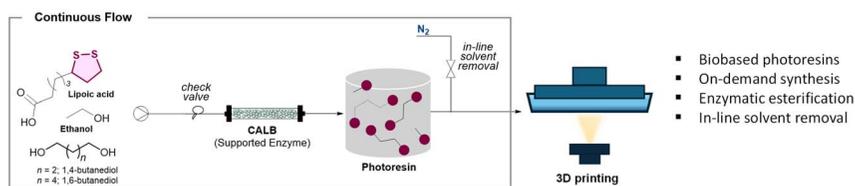

Fig. 1   On-demand photocurable resin synthesis under continuous flow conditions followed by off-line 3D printing developed in this work.

photocurable resins have been synthesised using a sustainable enzymatic esterification. The environmental feasibility of the circular resin production under continuous flow conditions was lastly assessed through life cycle assessment analysis, proving it to be a more sustainable strategy than the previously reported synthetic protocols.

Results and discussion

Enzymatic esterification under continuous flow conditions

Liquid resin formulations employed in 3D printing are usually made of a reactive diluent and multivalent crosslinkers. The reactive diluent, ethyl lipoate ($EtLp_1$) synthesis was carried out under continuous flow conditions (Table 1), exploring a range of solvents including dichloromethane (CH_2Cl_2), and greener ones, such as 2-methyl tetrahydrofuran (2-MeTHF) and methyl ethyl ketone (MEK). A single syringe system was used by combining ethanol (1.05 equiv.) and a solution of lipoic acid (LA) in CH_2Cl_2 (2.42 M). Initially, a packed-bed reactor was prepared using 0.5 g of supported Lipase B from *Candida antarctica* (CALB), and the reagents were flowed at a flow rate of 0.1 mL min^{-1}, resulting in a residence time of 25 minutes (see ESI† for details). Fractions of the $EtLp_1$ product were collected at 1 h intervals, and their composition was monitored using ^{1}H NMR spectroscopy. Under these conditions, a 65% $EtLp_1$ yield was detected when the steady state was achieved (Table 1, entry 1). To minimise the amount of the solvent employed in the process, the concentration of the solution was doubled; however, that led to a gelation of the solution within the reactor, making that condition impracticable for the production of photocurable resins (Table 1, entry 2).

Table 1 Screening of the reaction conditions for the enzymatic synthesis of $EtLp_1$ under continuous flow conditions[a]
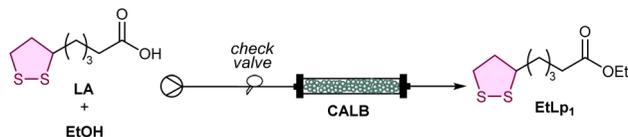
Entry	Catalyst/g	Solvent	Flow rate/mL min^{-1}	τ/min	$EtLp_1$/%
1	0.5	CH_2Cl_2	0.1	25	65
2[b]	0.5	CH_2Cl_2	0.1	25	—
3	0.8	CH_2Cl_2	0.1	35	88
4	0.8	CH_2Cl_2	0.07	50	94
5	0.8	2-MeTHF	0.07	40	70
6	0.8	2-MeTHF	0.05	65	85
7	0.8	MEK	0.07	50	73
8	0.8	MEK	0.05	80	72
9[c]	2.0	CH_2Cl_2	0.11	80	95
10[c]	2.0 + (0.5 g $MgSO_4$)	CH_2Cl_2	0.1	80	96

[a] Reaction conditions: LA (1 equiv.), EtOH (1.05 equiv.), solvent (2.42 M), CALB (x g), flow rate, rt. [b] Solvent (4.85 M). [c] EtOH (1.20 equiv.). τ stands for residence time.

To increase the conversion of LA into the corresponding $EtLp_1$, the catalyst amount and flow rate were then optimised. The catalyst amount was initially increased to 0.8 g, leading to an increased residence time of 35 min. Under these conditions, an 88% $EtLp_1$ yield was obtained using a 0.1 mL min^{-1} flow rate (Table 1, entry 3). The results observed were consistent with previously reported experiments on continuous esterification, as conversion enhancement is seen with increasing the catalyst bed height.[29] A further increase in $EtLp_1$ yield (94%) was achieved by lowering the flow rate to 0.07 mL min^{-1} (Table 1, entry 4).

With the aim of designing a sustainable and scalable esterification protocol, alternative green solvents with low boiling points were also explored. The use of 2-MeTHF as the solvent resulted in a lower $EtLp_1$ yield (70%, Table 1, entry 5) at a 0.07 mL min^{-1} flow rate, while a decrease to 0.05 mL min^{-1} led to an $EtLp_1$ yield of 85% (Table 1, entry 6). The use of 2-MeTHF led to reduced process efficiency, most likely a consequence of its inferior resin swelling properties compared to CH_2Cl_2, which in turn resulted in less effective mass transfer (Fig. S12 and S13†). MEK was also tested, achieving 73% $EtLp_1$ formation at room temperature with a 0.07 mL min^{-1} flow rate (entry 7, Fig. S14†). Decreasing the flow rate to 0.05 mL min^{-1} showed no improvement (Table 1, entry 8).

To explore the process scalability, a large-scale reactor was prepared with 2 g of supported enzyme. The scale-up was tested using CH_2Cl_2, and the results achieved were consistent with the small-scale experiments (Table 1, entry 9). Moreover, the use of drying agents (e.g., $MgSO_4$ or molecular sieves) to suppress ester hydrolysis during esterification yielded negligible improvement (Table 1, entry 10). Finally, to understand the stability of the developed system, a long-run experiment was performed. Fractions were collected every hour, and $EtLp_1$ formation was stable for 13 h, with more than 36 g of $EtLp_1$ produced in that time frame (Fig. 2a).

To explore the preparation of photocurable resins under flow conditions, multivalent crosslinkers were then synthesised following the same protocol used for the reactive diluent, $EtLp_1$. Previously reported lipoic acid-based crosslinkers[11] were initially targeted. Glycerol and sugar-based isosorbide and isomanide were tested; however, their enzymatic esterification at room temperature was inefficient. Hence, alternative biobased alcohols, 1,4-butanediol and 1,6-hexanediol, were considered.[30,31] The synthesis of the hexyl lipoate derivative ($HexLp_2$) was carried out by combining 1,6-hexanediol (1 equiv.) and a solution of LA in CH_2Cl_2 (2.42 M). Reagents were initially supplied at a flow rate of 0.1 mL min^{-1} and fractions were collected at 1 h intervals and analysed using ^1H NMR spectroscopy. Under these conditions, $HexLp_2$ was obtained with an 86% yield (Fig. 2b), while using a flow rate of 0.08 mL min^{-1} was shown to lead only to a slightly higher yield (89%). Lastly, decreasing the flow rate to 0.05 mL min^{-1} showed consistent data with higher flow rates, with only a marginal increase in yield (90% yield of $HexLp_2$).

Subsequently, the synthesis of butyl lipoate ester ($ButLp_2$) was carried out under flow conditions using the same conditions optimised for $HexLp_2$ by combining 1,4-butandiol (1 equiv.) and a solution of LA in CH_2Cl_2 (2.42 M). Using a large-scale reactor (with 2 g of supported enzyme) with a flow rate of 0.1 mL min^{-1} led to $ButLp_2$ being obtained with an 84% yield when the steady state was reached (Fig. 2c).
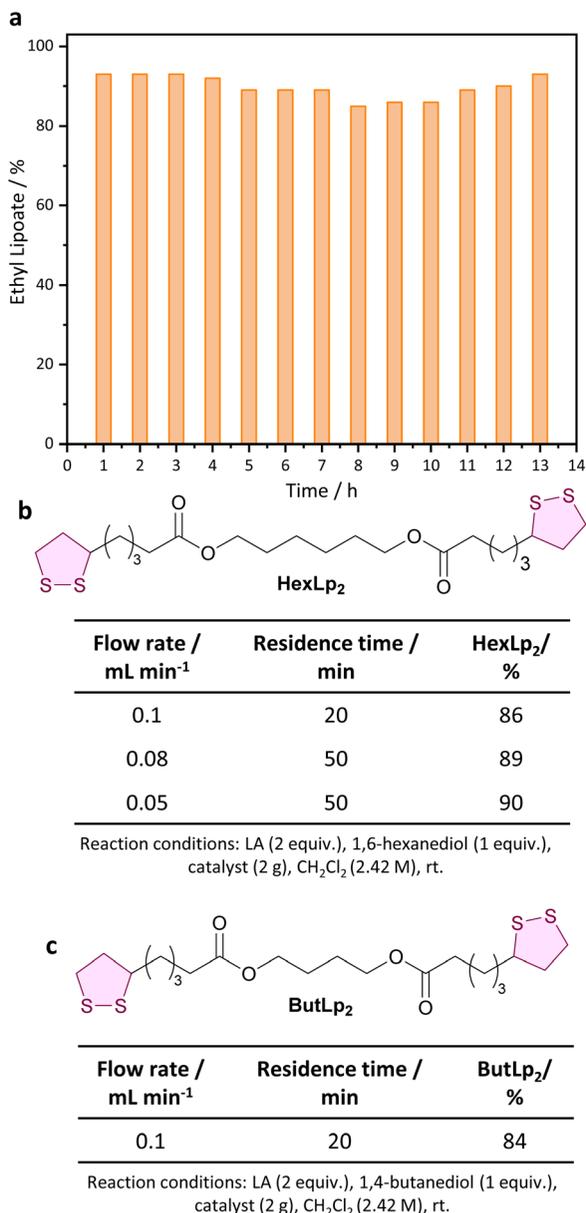
Fig. 2 (a) EtLp$_1$ long-run continuous flow preparation (reaction conditions: Table 1, entry 4). (b) Screening of the reaction conditions for the enzymatic synthesis of multivalent crosslinkers HexLp$_2$. (c) Reaction conditions for the enzymatic synthesis of multivalent crosslinkers ButLp$_2$.

b HexLp$_2$

Flow rate / mL min^{-1}	Residence time / min	HexLp$_2$/ %
0.1	20	86
0.08	50	89
0.05	50	90

Reaction conditions: LA (2 equiv.), 1,6-hexanediol (1 equiv.), catalyst (2 g), CH$_2$Cl$_2$ (2.42 M), rt.

c ButLp$_2$

Flow rate / mL min^{-1}	Residence time / min	ButLp$_2$/ %
0.1	20	84

Reaction conditions: LA (2 equiv.), 1,4-butanediol (1 equiv.), catalyst (2 g), CH$_2$Cl$_2$ (2.42 M), rt.

Photocurable resin preparation under continuous flow conditions

Photopolymer resins were prepared by combining the reactive diluent (EtLp$_1$) and multivalent crosslinker (HexLp$_2$ or ButLp$_2$) made by continuous flow enzymatic esterification (Fig. 3a). EtLp$_1$ and HexLp$_2$ were both prepared under continuous
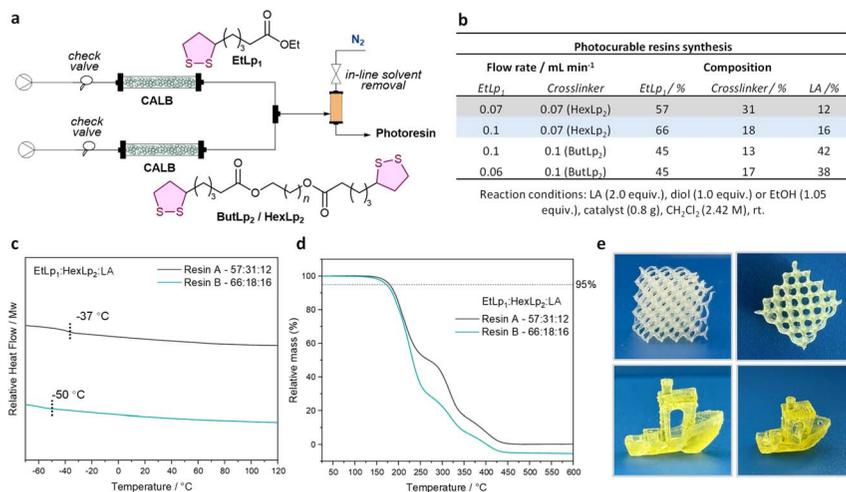
Fig. 3 (a) Continuous flow set-up for photocurable resin preparation. (b) Composition of the combined photocurable resin obtained under continuous flow conditions. (c) DSC thermograms of the second heating cycle of the $EtLp_1 : HexLp_2$ resins (−80 to 130 °C, 10 °C min^{-1} under N_2). T_g is indicated by the dashed line. (d) TGA thermograms of the $EtLp_1 : HexLp_2$ resin 2D-photoset post-cured samples (25–600 °C, N_2 atmosphere). $T_{d5\%}$ is indicated by a horizontal line. (e) 3D-printed complex parts, top and front views.

flow conditions in separate flow reactors, each packed with the supported enzyme (0.8 g) and initially set to a flow rate of 0.07 mL min^{-1}. The outlet of each reactor was connected at a T-junction, and the mixed photocurable resin was collected in a separating funnel. Nitrogen was bubbled through the collected solution while the resin was being prepared to ensure that the final product had minimal solvent content for the following printing process. Aliquots were taken at 1 h intervals and the ratios of $EtLp_1$, $HexLp_2$ and lipoic acid of the combined resin were determined using ^{1}H NMR spectroscopy. As lipoic acid is not fully converted into the ester derivative, we anticipated that the unreacted LA could be incorporated into the material when photocured.

To determine whether the composition of the resin could be tuned *via* the continuous flow parameters, the flow rate of the $EtLp_1$ process was increased from 0.07 mL min^{-1} to 0.1 mL min^{-1}. It was hypothesised that increasing the flow rate would result in a higher amount of $EtLp_1$ as there would be a higher volume of $EtLp_1$ in the combined resin compared to $HexLp_2$. On the other hand, increasing the flow rate would also increase the amount of lipoic acid in the final photocurable resin as a lower conversion of $EtLp_1$ would be achieved with the lower residence time. The resulting resin composition showed that increasing the flow rate of $EtLp_1$ does lead to an increase in the amount of $EtLp_1$ and lipoic acid in the final resin and a decrease in the amount of the crosslinker $HexLp_2$ (Fig. 3b). In doing so, we demonstrated that changing the continuous flow parameters enables the final resin composition to be tuned. This represents a novel approach to tune photocurable resin compositions and therefore prepare on-demand tailored photocurable resins in an automated way. Similarly, a $EtLp_1 : ButLp_2 :$ LA photocurable resin was prepared with an analogous set-up. Due to the higher

flow rates employed relative to the $EtLp_1 : HexLp_2$ resin preparation, the $EtLp_1 :$ $ButLp_2$ resin exhibited an increased lipoic acid content (Fig. 3b). This outcome was anticipated as higher flow rates result in lower conversions.

To explore the material properties of the $EtLp_1 : HexLp_2 : LA$ photopolymer resins, 2D photosets of the resins were prepared by curing 0.1 mL of resin on glass slides (10 min UV irradiation), followed by post-curing for 24 h at 60 °C (Fig. S15†). Differential scanning calorimetry (DSC) and thermogravimetric analysis (TGA) of the obtained photocured polymers were conducted. The glass transition temperature (T_g) for the resin containing a 57 : 31 : 12 ratio of $EtLp_1 : HexLp_2 : LA$ (resin A) was −37 °C, whereas the T_g for the resin containing a 66 : 18 : 16 ratio of $EtLp_1 : HexLp_2 : LA$ (resin B) was −50 °C (Fig. 3c). The difference in T_g can be ascribed to the higher content of $HexLp_2$ crosslinker, which leads to a higher degree of crosslinking. This proof-of-concept experiment shows that the material properties of the resins can be tuned by preparing the photopolymer resins under flow conditions. Lastly, both resins showed thermal stability up to 170 °C (Fig. 3d), in line with lipoic acid-based photopolymers previously reported.[11]

To explore the structure–property space of the platform, additional samples of the resin were prepared using $ButLp_2$. However, we observed a partial gelation of the formulated photocurable resin as soon as the solvent was removed, which proved to be unsuitable for the following application in additive manufacturing.

Printing the resin $EtLp_1 : HexLp_2 : LA$ (57 : 31 : 12) on a commercial digital light processing (DLP) printer was achieved using a $\lambda = 405$ nm light source (Fig. 3e). The high-fidelity, complex prints were obtained using a 35 s cure per layer, which corresponds to a build rate of 5.1 mm h^{-1} (excluding the peeling time process), demonstrating that the resins prepared through the continuous flow method remained suitable for DLP printing.

life cycle assessment and green chemistry metrics

A first estimation of the sustainability of the preparation of circular lipoic acid-based resins was explored using green chemistry metrics (Table S1†). The enzymatic reaction is considered to be a more sustainable approach, with chemicals such as N-(3-dimethylaminopropyl)-N'-ethylcarbodiimide (EDC), commonly used in esterification reactions, replaced by the supported enzyme. Additionally, the continuous flow approach minimises the purification process, limiting it to the sole solvent removal. For the proposed enzymatic process, the atom economy (AE)[32] was equal to 93, meaning that most of the reagents are converted into the products with little waste production. In contrast, the previously used EDC coupling[11] pathway (here named as petrochemical process) resulted in a significantly lower value as a consequence of the high amount of waste produced and the lower efficiency of the process (78% yield for the petrochemical process vs. 94% for the enzymatic process). The E factor[33] for the enzymatic process was calculated to be <0.01, falling into the range of oil refinery processes, while it is equal to 2.57 when the solvent is considered, showing a comparable value with the recently reported Fisher esterification process.[34] The use of EDC led to a higher E factor (17.04 when the solvent is considered, Table S1†), comparable with those of bulk processes. While these parameters showed that the enzymatic process is more sustainable than the petrochemical one, an absolute assessment of the process sustainability must take into account the energy required for the

Faraday Discussions

reaction, as well as the impact of the production of the chemicals that are needed for the reactions themselves. Hence, to obtain a comprehensive understanding of the real sustainability of both reaction pathways, a life cycle assessment (LCA) that compares the two synthetic protocols was performed.

The LCA carried out conformed to the existing ISO standard (14044) and followed the typical LCA framework.[35] The LCA system boundary consisted of raw materials and chemical supply, and electricity (Fig. 4a). Material and chemical flows are depicted according to these working schemes (Fig. 4b). Outputs were not reused; all outputs were either transferred to the next process or, if not intended, considered as waste. The waste products from the system included by-products, aqueous solutions and solid waste for which the impacts were not considered.

This LCA has a cradle-to-gate attributional approach and did not include any infrastructure processes related to lab equipment production (see ESI† for details). The background data used for basic chemicals, such as solvents and reagents, comes from the Ecoinvent-3 database. Lipoic acid is not included in the Ecoinvent-3 database used; therefore, it was replaced with the fatty acid, stearic acid. The amount of ester obtained for the petrochemical and enzymatic processes was obtained from experimental data, and the reaction conditions were adjusted to synthesise 100 g of ethyl ester. The petrochemical process was divided into two sub-processes: the synthetic one and the purification step. The enzymatic process instead did not require any purification, aside from solvent removal under vacuum and was therefore considered as a sole process. Finally, we considered the flow system to operate for 35 h to allow the preparation of 100 g of ethyl ester, assuming a steady-state regime.

In this study, midpoint indicator assessment was conducted using ReCiPe 2016 Endpoint (E) V1.08 to better understand and compare the impact
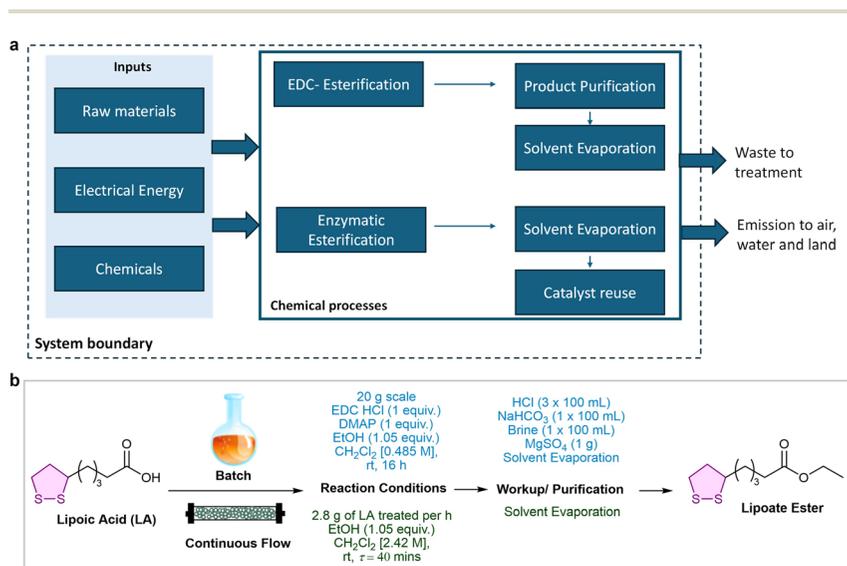

Fig. 4 (a) System boundary for life cycle analysis of lipoic acid esterification. (b) Materials flow scheme for reaction procedure for both the petrochemical esterification under batch conditions and enzymatic esterification under continuous flow conditions, divided into two phases by reaction and workup/purification.

categories.[36] The LCA of petrochemical esterification was conducted based on two stages in the inventory analysis: the synthetic process and the purification (removal of unreacted reagents and by-products) process. The waste treatment processes and emissions to air, water and land were not considered as part of the LCA.

Relative results were generated from the simulation for which the indicator results maximum is set to 100% (Fig. 5 and Table S3†). The petrochemical synthetic process is above the purification process in all the categories. When compared to the enzymatic process, the petrochemical synthesis is still above the purification and the enzymatic synthesis in all categories.

The petrochemical esterification process had the highest environmental impact across all criteria, mainly due to its long reaction time, high solvent use, and toxic reagents like EDC. The workup stage also contributed significantly, primarily through waste generation. In contrast, the enzymatic process showed the lowest impact, benefiting from a biobased catalyst, lower energy use, and more concentrated solutions that reduced solvent removal energy demands. Water consumption in the petrochemical process was 0.099 m^3 per unit of product, while the continuous flow method used only 0.002 m^3, reducing water usage by over 90% thanks to more efficient reagent use and simpler purification. Land system changes were also significantly lower in the continuous flow process (0.002 m^2 vs. 0.061 m^2 per unit), mainly due to reduced solvent and reagent requirements. Carbon emissions were over 95% lower in the enzymatic process compared to the petrochemical route, highlighting the environmental benefits of using a syringe pump instead of a stirring plate. Across all nine planetary boundaries, including ocean acidification, biosphere integrity, and freshwater use, the enzymatic approach showed the least impact. The petrochemical method had the highest toxicity, largely due to chlorinated reagents and solvents.
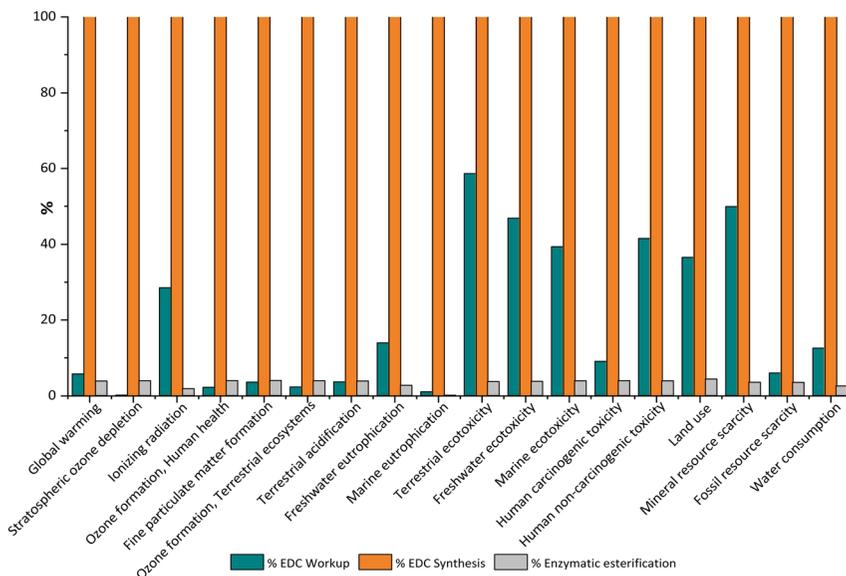

Fig. 5 Environmental impacts due to the synthesis of 100 g of ethyl ester computed using ReCiPe 2016 V1.08.

Faraday Discussions

Lastly, ReCiPe 2016 Endpoint (E) V1.08 was used to conduct endpoint analysis. Human health, ecosystem quality and resources endpoint indicator assessments have been compared for the petrochemical and enzymatic processes (Fig. 6). Ecosystem quality comprises acidification, ecotoxicity, eutrophication and land use (indicated as species × year ["Species*yr"]). Human health is related to the impacts of environmental degradation that increases the number and duration of loss-of-life-related diseases (recorded as disability-adjusted life year (DALY)). For resources, it is closely related to the depletion rate of raw materials and energy sources (recorded as extra costs in US dollars for future mineral and fossil resource extraction (USD)). Results are evaluated based on the future energy surplus requirements needed to produce lower-quality energy and minerals. For all the categories, the enzymatic esterification showed a lower impact than the petrochemical process (Fig. 6b). By combining the precise midpoint results with the aggregated endpoint outcomes, we provided a robust and comprehensive assessment of the environmental performance of the seven processes, capturing both detailed category-specific impacts and their broader environmental effects. In summary, the implementation of the enzymatic esterification under continuous flow conditions resulted in the reduction of more than 90% based on the average outcomes observed in the respective categories of the endpoint method.

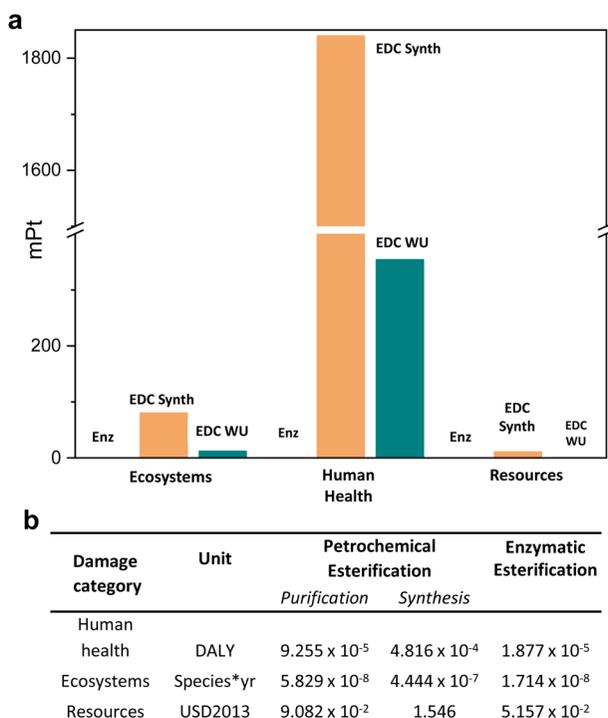| Damage category	Unit	Petrochemical Esterification		Enzymatic Esterification
		Purification	Synthesis	
Human health	DALY	9.255×10^{-5}	4.816×10^{-4}	1.877×10^{-5}
Ecosystems	Species*yr	5.829×10^{-8}	4.444×10^{-7}	1.714×10^{-8}
Resources	USD2013	9.082×10^{-2}	1.546	5.157×10^{-2}

Fig. 6 (a) ReCiPe 2016 Endpoint (E) V1.08 endpoint indicators for producing 100 g of ethyl ester. 'Enz' stands for enzymatic synthesis, 'EDC synth' stands for petrochemical synthesis, and 'EDC WU' represents the workup step for the petrochemical esterification. (b) Environmental impacts due to the stearic acid esterification process (100 g) computed using ReCiPe 2016 Endpoint (E) V1.08.

Conclusions

These results demonstrate a proof-of-concept advancement in developing a continuous flow system for the sustainable production of circular, biobased photocurable resins. Enzymatic esterification under continuous flow conditions enabled the on-demand synthesis of lipoate-based photocurable resins with tuneable compositions. The integration of in-line solvent removal streamlined the process, yielding one-step, printable resins that can be directly utilised in DLP printing. By employing renewable, sustainable, and non-hazardous lipoates, this approach effectively overcomes major limitations of current state-of-the-art resins and demonstrates significant potential for broader implementation. Finally, the sustainability of the method was further assessed through life cycle assessment. Overall, the study reaffirms the effectiveness of continuous enzymatic flow synthesis in enhancing environmental performance across multiple areas, from human health to ecosystem impact and resources. Future work will focus on expanding the library of on-demand photocurable resins and developing an integrated one-pot online printing process.

Data availability

The data supporting this article have been included as part of the ESI.†

Author contributions

A. B. and A. P. D. conceived the work. All authors designed the experiments. N. N. M., D. G., M. R. E. and A. B. performed and analysed the experiments. N. M. aided in the LCA. A. B. directed the research and prepared the manuscript. All authors contributed to manuscript revisions and have given approval to the final version of the manuscript.

Conflicts of interest

There are no conflicts to declare.

Acknowledgements

Notes and references

1 F. Zhang, L. Zhu, Z. Li, S. Wang, J. Shi, W. Tang, N. Li and J. Yang, *Addit. Manuf.*, 2021, **48**, 102423.
2 S. C. Ligon, R. Liska, J. Stampfl, M. Gurr and R. Mülhaupt, *Chem. Rev.*, 2017, **117**, 10212–10290.
3 **https://www.grandviewresearch.com/industry-analysis/photopolymers-market-report**.
4 I. Gibson, D. Rosen, B. Stucker, M. Khorasani, D. Rosen, B. Stucker and M. Khorasani, *Additive Manufacturing Technologies*, Springer, 2021.

5   V. S. Voet, J. Guit and K. Loos, *Macromol. Rapid Commun.*, 2021, **42**, 2000475.

6   W. Li, L. S. Mille, J. A. Robledo, T. Uribe, V. Huerta and Y. S. Zhang, *Adv. Healthcare Mater.*, 2020, **9**, 2000156.

7   M. Bachmann, C. Zibunas, J. Hartmann, V. Tulus, S. Suh, G. Guillén-Gosálbez and A. Bardow, *Nat. Sustain.*, 2023, **6**, 599–610.

8   X. Lopez de Pariza, O. Varela, S. O. Catt, T. E. Long, E. Blasco and H. Sardon, *Nat. Commun.*, 2023, **14**, 5504.

9   P. Chakma and D. Konkolewicz, *Angew. Chem., Int. Ed.*, 2019, **58**, 9682–9695.

10 G. Zhu, H. A. Houck, C. A. Spiegel, C. Selhuber-Unkel, Y. Hou and E. Blasco, *Adv. Funct. Mater.*, 2024, **34**, 2300456.

11 T. O. Machado, C. J. Stubbs, V. Chiaradia, M. A. Alraddadi, A. Brandolese, J. C. Worch and A. P. Dove, *Nature*, 2024, **629**, 1069–1074.

12 B. Zhang, K. Kowsari, A. Serjouei, M. L. Dunn and Q. Ge, *Nat. Commun.*, 2018, **9**, 1831.

13 M. Podgórski, S. Huang and C. N. Bowman, *ACS Appl. Mater. Interfaces*, 2021, **13**, 12789–12796.

14 H. Gao, Y. Sun, M. Wang, Z. Wang, G. Han, L. Jin, P. Lin, Y. Xia and K. Zhang, *ACS Appl. Mater. Interfaces*, 2021, **13**, 1581–1591.

15 J. J. Hernandez, A. L. Dobson, B. J. Carberry, A. S. Kuenstler, P. K. Shah, K. S. Anseth, T. J. White and C. N. Bowman, *Macromolecules*, 2022, **55**, 1376–1385.

16 B. Yang, T. Ni, J. Wu, Z. Fang, K. Yang, B. He, X. Pu, G. Chen, C. Ni and D. Chen, *Science*, 2025, **388**, 170–175.

17 E. Yang, S. Miao, J. Zhong, Z. Zhang, D. K. Mills and L. G. Zhang, *Polym. Rev.*, 2018, **58**, 668–687.

18 S. Subedi, S. Liu, W. Wang, S. A. Naser Shovon, X. Chen and H. O. T. Ware, *npj Adv. Manuf.*, 2024, **1**, 9.

19 A. Jadhav and V. S. Jadhav, *Mater. Today: Proc.*, 2022, **62**, 2094–2099.

20 R. Tu and H. A. Sodano, *Addit. Manuf.*, 2021, **46**, 102180.

21 C. C. Cook, E. J. Fong, J. J. Schwartz, D. H. Porcincula, A. C. Kaczmarek, J. S. Oakdale, B. D. Moran, K. M. Champley, C. M. Rackson and A. Muralidharan, *Adv. Mater.*, 2020, **32**, 2003376.

22 N. Zaquen, M. Rubens, N. Corrigan, J. Xu, P. B. Zetterlund, C. Boyer and T. Junkers, *Prog. Polym. Sci.*, 2020, **107**, 101256.

23 A. Laybourn, K. Robertson and A. G. Slater, *J. Am. Chem. Soc.*, 2023, **145**, 4355–4365.

24 S. B. Patterson, R. Wong, G. Barker and F. Vilela, *J. Flow Chem.*, 2023, **13**, 103–119.

25 M. H. Reis, F. A. Leibfarth and L. M. Pitet, *ACS Macro Lett.*, 2020, **9**, 123–133.

26 M. B. Plutschack, B. U. Pieber, K. Gilmore and P. H. Seeberger, *Chem. Rev.*, 2017, **117**, 11796–11893.

27 F. Fanelli, G. Parisi, L. Degennaro and R. Luisi, *Beilstein J. Org. Chem.*, 2017, **13**, 520–542.

28 M. B. Montaner and S. T. Hilton, *Curr. Opin. Green Sustainable Chem.*, 2024, **47**, 100923.

29 Y. Feng, A. Zhang, J. Li and B. He, *Bioresour. Technol.*, 2011, **102**, 3607–3609.

30 H. Kim, S. Lee and W. Won, *Energy*, 2021, **214**, 118974.

31 H. Guo, H. Liu, Y. Jin, R. Zhang, Y. Yu, L. Deng and F. Wang, *Biochem. Eng. J.*, 2022, **185**, 108478.

32 P. Anastas and N. Eghbali, *Chem. Soc. Rev.*, 2010, **39**, 301–312.

33 R. A. Sheldon, *Green Chem.*, 2007, **9**, 1273–1283.

34 C. Koelbl, C. Obunadike, W. Ham, N. Mahmud, M. Garcia, E. Lizundia and J. C. Worch, *ChemSusChem*, 2025, 202500194, DOI: **10.1002/cssc.202500194**.

35 I. Iso, *Environmental Management—Life Cycle Assessment—Requirements and Guidelines*, 2006, pp. 1–46.

36 M. A. Huijbregts, Z. J. Steinmann, P. M. Elshout, G. Stam, F. Verones, M. Vieira, M. Zijp, A. Hollander and R. Van Zelm, *Int. J. Life Cycle Assess.*, 2017, **22**, 138–147.